Microscopic mechanisms of initial oxidation of Si(100): Reaction pathways and free-energy barriers

Kenichi Koizumi,[1,*] Mauro Boero,[2] Yasuteru Shigeta,[3] and Atsushi Oshiyama[1]

[1]*Department of Applied Physics, The University of Tokyo, Hongo, Tokyo 113-8656, Japan*
[2]*IPCMS, UMR 7504 CNRS and University of Strasbourg, F-67034 Strasbourg 2, France*
[3]*Department of Materials Engineering Science, Osaka University, Toyonaka, Osaka 560-8531, Japan*

Various reaction pathways and corresponding activation barriers in the initial oxidation of Si(100) surfaces are clarified by free-energy sampling techniques combined with the Car-Parrinello molecular dynamics. We find a crucial stable geometry which is ubiquitous during the oxidation and links the dissociation of O_2 molecules and the oxidation of subsurfaces. The calculated free-energy landscape provides a comprehensive picture of the various competing reaction pathways.

I. INTRODUCTION

Oxygen is ubiquitous on earth and oxidation of materials is common in human life. The understanding of the oxidation process is thus fundamental to our knowledge of nature. In various stages in technology ranging from cutting edge miniaturization of semiconductor devices[1,2] to biocompatible applications,[3] oxide films of silicon are widely utilized to fabricate complex structures and also to generate functions of devices. In current semiconductor technology,[4] the thickness of Si oxide becomes less than 1 nm and a new class of materials named high k is combined with Si oxide to ensure its durability.[4–6] It is thus mandatory to get a comprehensive atomic-level insight into the mechanisms of the oxidation in order to clarify and tune the properties of the oxide films.

After several pioneering theoretical works,[7–9] a realistic atomic-level insight about the Si oxidation was given by Kato and coworkers.[10,11] Their static density-functional calculations have shown that oxidation of the Si(100) surface proceeds via backbond oxidation. Recently, Ciacchi and Payne revisited the Si(100) oxidation process via first-principles molecular dynamics (FPMD) in the *NVE* ensemble.[12] Their results indicate a different thermally activated mechanism for the backbond oxidation, underscoring the importance of dynamical study. For the atomistic understanding of the oxidation process, however, it is imperative to identify reaction pathways for dissociation of oxygen molecules and then formation of Si-O bonds, and furthermore to obtain the corresponding free-energy barriers. Since the typical barrier is about a half eV or more, it is difficult to simulate these elementary processes by standard FPMD methods.

To resolve the difficulty, we here investigate the reaction mechanisms of the initial oxidation processes on Si(100) by Car-Parrinello molecular dynamics (CPMD) simulations[13] combined with the blue moon (BM) ensemble[14] and the metadynamics (MTD) free-energy sampling approaches,[15,16] which have been shown to possess accuracy and versatility in a wide range of applications.[17,18] We find a crucial configuration which links the dissociation of O_2 molecules and further oxidation of subsurfaces. Detailed reaction pathways and corresponding free-energy barriers are provided for the first time.

II. CALCULATIONS

In the calculations, valence electrons are expanded in the plane-wave basis set with an energy cutoff of 70 Ry and the core-valence interaction is described by norm-conserving pseudopotentials.[19] All simulations are done within the generalized gradient approximation[20] with a spin-unrestricted approach. The Si(100) surface is modeled by a slab of six Si layers and the exposed area corresponds to a $c(4 \times 4)$ surface, wide enough to allow for a sampling of the Brillouin zone to the Γ point only. Above the surface a vacuum space of 8.6 Å allows for a good separation of repeated images of the simulation cell. The ionic temperature is controlled by Nosé-Hoover thermostat[21] in *NVT* simulations.

III. RESULTS AND DISCUSSION

A. Reaction pathways described by metadynamics

We have first examined various configurations of an O_2 molecule on Si(100) via unconstrained *NVT* simulations at 300 K, since experiments suggest an initial oxidation occurring at room temperature.[22] Our results confirm the findings of Ref. 11 within an error bar of 1%: namely an O_2 dissociation energy of 5.66 eV and an adsorption energy of O_2 to a Si dimer at the Si(100) of 2.92 eV. We have then investigated the dissociation of O_2 from the most probable O_2 configuration in which both O atoms are absorbed on top of a dimer [the minimum (A) configuration of Fig. 1(c)] by using MTD. To this aim, we use two different sets of collective variables (CVs) in our MTD simulations. In the first case, the CVs are the two distances between each of the two O atoms and the center of the closest Si-Si bond in the first layer, as shown in Fig. 1(a). In the second case, the two CVs are the distances between each of the two O atoms and the nearest Si atoms belonging to the first layer [Fig. 1(b)]. Each MTD simulation lasted for about 70 ps, to ensure a good convergence of the free-energy sampling as specified in Ref. 23. Both simulations result essentially in an identical reaction pathway. Specifically, the chemical bond between the two O atoms is cleaved and the O atom bound to the upper Si atom of the Si-Si dimer moves toward the backbond site. Simultaneously, the second O atom is displaced very rapidly into the on-dimer site, as shown in the minimum (B) configuration of Fig. 1(c). This process can be
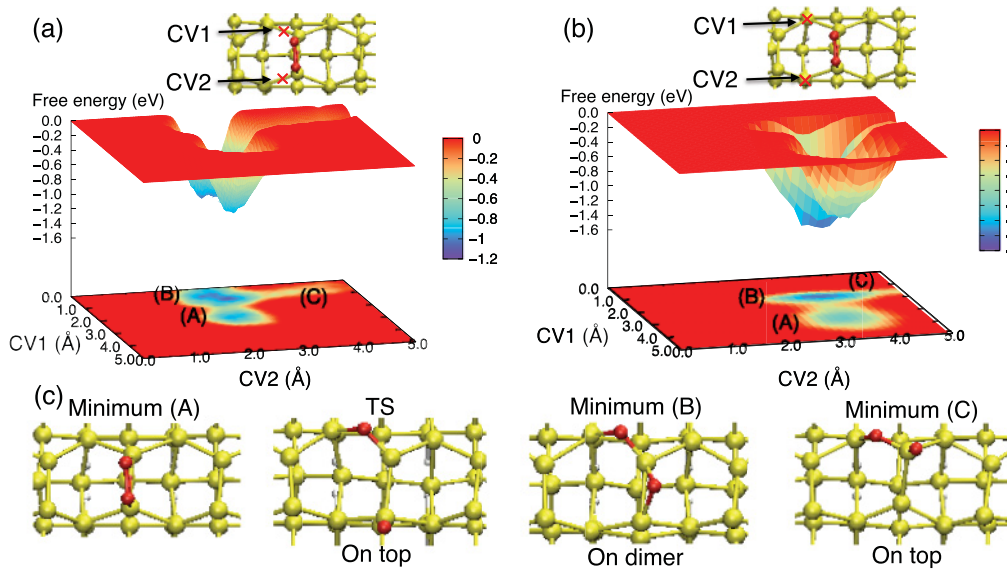
FIG. 1. (Color online) Free-energy landscapes obtained by MTD simulations and related stable configurations [Si: yellow (light gray), O: red (dark gray)]. (a) Distances of each O atom from each center of the backbonds, shown as a red ×, are used as collective variables (CVs). (b) Distances of each O atom from the Si atom in the first layer, marked by a red ×, are used as CVs. (c) Structures of each local minimum and transition state (TS) for these reaction pathways. The relative free-energy difference between the minima (A) and (B) is not determined since the reverse reaction from (B) to (A) has not been simulated: Note that the free-energy landscape in MTD simulations is obtained from the history-dependent potential added to overcome the reaction barrier.

summarized as an escape from the initial free-energy minimum (A) to the next minimum (B). Our MTD simulations identify the transition state (TS) [TS in Fig. 1(c)], and the calculated free-energy barrier is $\Delta F(\text{TS-A}) = 0.43$ eV and $\Delta F(\text{TS-A}) = 0.55$ eV, respectively, in the two MTD simulations. This is the first determination of the free-energy barrier of the dissociation of an O_2 molecule. In terms of the total energy, the minimum (B) is more stable than the minimum (A) by about 3.50 eV, indicating that the initial dissociation process is exothermic.

We have found another metastable minimum, indicated as the minimum (C) in Fig. 1, which is characterized by a free-energy barrier of $\Delta F = 0.76$ eV in Fig. 1(a) and $\Delta F = 0.84$ eV in Fig. 1(b) with respect to the minimum (B). In this minimum (C), the O formerly in the on-dimer site is dislodged to the on-top site of the Si whose backbond is already oxidized. During the MTD simulations, the system visited a few times this metastable state (C) before settling down to the stable configuration (B). Reactions on the free-energy surface shown in Fig. 1(a) substantially differ from that speculated in Ref. 10.

B. Reaction pathways described by blue moon ensemble

We then explore the free-energy barrier for the back-bond oxidation starting from the minimum (B) configuration. Since in this case a single CV is sufficient, we use a BM approach in which the distances from the on-dimer O to the Si atom whose backbond is either oxidized or unoxidized are chosen as the two reaction coordinates (RCs). When the former RC is increased, one of the Si-O chemical bonds is cleaved and the O atom is displaced into the on-top site labeled (D) in Fig. 2(a). The barrier for this reaction is $\Delta F = 1.10$ eV.

When the latter RC is increased, the O atom is displaced into the on-top site labeled (C) in Fig. 2(a) [equivalent to (C) in Fig. 1(c)]. Pathways similar to these ones were investigated by the static calculations of Uchiyama and coworkers.[24] However, that static approach did not allow observation of the asymmetry in the pathways and free energies evidenced by our dynamical approach.

To seek further possible reaction pathways, we start other BM simulations from the geometries (C) and (D). Starting from (D), we introduce two RCs which measure the distance from the on-top O atom to one of the midpoints of the backbonds. The free-energy profiles along these RCs are shown by solid lines in Fig. 2(b). In both cases, the on-top O is inserted in the backbond with the free-energy barriers of $\Delta F = 0.31$ eV and $\Delta F = 0.51$ eV, respectively. Starting from (C), we introduce a RC which is the distance between the oxygen atom on the Si dimer and the midpoint of the Si-Si backbond. The free-energy profile along this RC is shown by a dotted line in Fig. 2(b). Along the RC, there is a shallow stable state [(E) in Fig. 2(b)] in which the on-top O sinks into the Si layer and bridges the two Si atoms. We refer to this as the "bridge" structure. The reaction from the bridge structure to the backbond configuration shown in Fig. 2(b) is unlikely.

We have now established that the insertion of the on-top O to the backbond requires high free-energy barriers of more than 1 eV. On the other hand, the reverse reaction in which the O atom at the on-top site goes back to the on-dimer site turned out to be almost barrierless. This is a stringent confirmation of our MTD results, in which O atoms in the on-top site refrain from getting into the backbond sites, but remain near the on-dimer site. This feature could not be unraveled in former calculations.[10,11]
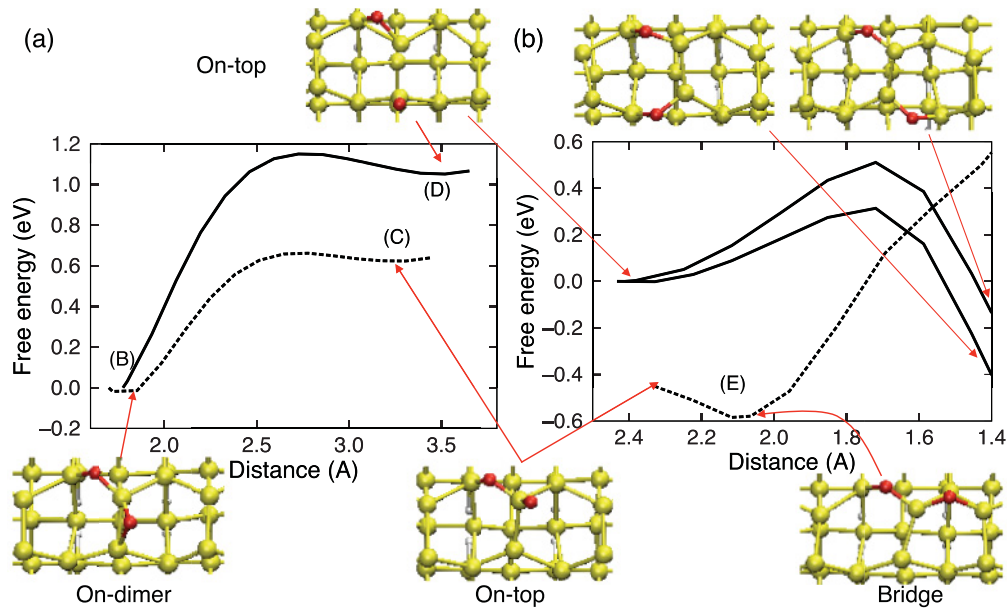
FIG. 2. (Color online) Free-energy profiles of the backbond oxidation calculated by BM approach. Pathways and corresponding free-energy profiles between the on-dimer geometry and the on-top geometry (a) and from the on-top geometry to the backbond oxidized geometry (b). The various panels show the geometries of the local minima (see text). Color code for atoms is the same as in Fig. 1.

C. Thermally activated dissociation of O_2

In a recent Letter,[12] Ciacchi and Payne suggested a pathway to backbond oxidation alternative to the one by Kato.[10,11] They have placed an O_2 molecule along the dimer row, performed *NVE* dynamics, and observed in some cases a thermally activated dissociation of the adsorbed O_2 adduct and a consequent backbond oxidation. To get a comprehensive picture, we have further examined the possibility of an O_2 molecule approaching the backbonds between the first- and the second-layer Si atoms which are exposed between dimer rows by using the BM approach. We have found that the O_2 molecule is attracted to the Si dimer and dissociates following a reaction path similar to the above thermally activated path.

From our MTD and BM simulations described above, we have identified a crucial stable structure, i.e., the minimum (B) configuration, which is stabilized against further reactions by a free-energy barrier of 1 eV. Thus it is highly expected that the geometry (B) is ubiquitous in the initial stage of the oxidation. Hence, in order to explore the next step of the oxidation, we prepare a pair of the minimum (B) configurations, place an O_2 molecule, and perform unconstrained *NVT* simulations at 300 K.

The starting geometries we examine are shown in Figs. 3(a) and 3(c): namely, two possible pairs of the minimum (B) configurations plus attacking O_2 molecules. In the optimized starting structure, spin densities are distributed both on the O_2 moiety and on the Si surface, as shown in Fig. 4(a). The highest occupied (HO) and the lowest unoccupied (LU) Kohn-Sham orbitals (KOs) are also shown in Fig. 4. It is noteworthy that HOKOs have a character of an antibonding orbital, π^*, of the attacking O_2 molecule. This indicates that the electron is dragged from the Si surface to the O_2 moiety where the O-O bond becomes weak. We also find that the π^* component of the spin-up HOKO is oriented parallel to the Si surface, whereas those of the spin-down HOKO and

the spin-up LUKO are orthogonal to the surface, indicating higher acceptability of electrons.

The bond weakening of the O_2 moiety due to the electron transfer (Fig. 4) promotes the dissociation of the O_2. Our unconstrained dynamics indeed reveals that the starting geometries shown in Figs. 3(a) and 3(c) evolve to the next geometries in 2 ps, shown in Figs. 3(b) and 3(d), respectively, in which one O of the O_2 moiety intervenes in the nearby Si-Si backbond. The final oxidized configurations, shown in Figs. 3(b) and 3(d), are lower in the total energy than the corresponding starting geometries by 4.5 eV.

An interesting finding during these oxidation processes is the fact that the Si-Si bond of the dimer to which the O atom is adsorbed starts to break apart and an electron
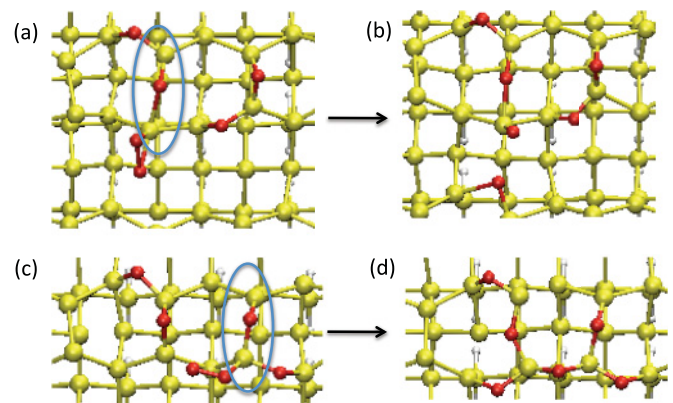
FIG. 3. (Color online) Thermally activated backbond oxidation in pairs of minimum (B) configurations. The oxidation proceeds from (a) to (b), or (c) to (d). In both cases, an O of the O_2 intervenes in the backbond whereas the other O stays near the on-top site. Si dimer bonds are broken as circled in (a) and (c). Color code for atoms is the same as in Fig. 1.
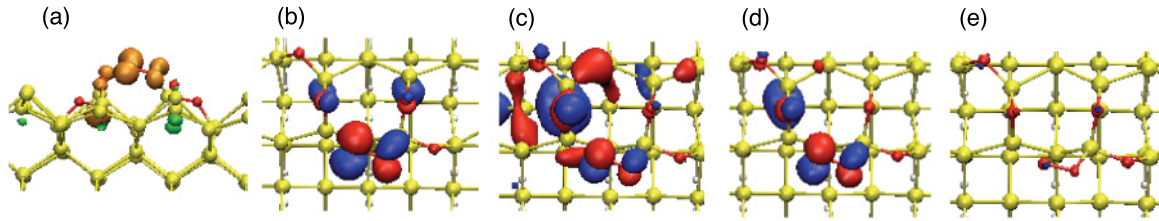
FIG. 4. (Color online) Spin density (a), spin-up HOKO, (c) spin-down HOKO, (d) spin-up LUKO, and (e) spin-down LUKO in the pair of minimum (B) configuration plus an O_2 shown in Fig. 3(c). In (a), the isosurfaces at $\pm 2 \times 10^{-3}$ $e/\text{Å}^3$ are shown in orange (light gray) and green (dark gray), respectively. From (b) to (e), the isosurfaces at $\pm 2.4 \times 10^{-2}$ $(e/\text{Å}^3)^{1/2}$ are shown in red (dark gray) and blue (black), respectively. Color code for atoms is the same as in Fig. 1.

transfer occurs from the Si-Si bond to O_2. As shown by circles in Fig. 3(a) and 3(c), this bond cleavage causes a rather free motion of surrounding atoms, thus causing flexible relaxation that promotes the backbond oxidation even to neighboring dimer rows [Fig. 3(b)]. Dynamical simulations within the BM approach have shown that the free-energy barrier corresponding to the reaction bringing the on-top configuration of Fig. 3(b) to the backbond site is about 0.45 eV.

We have found that an oxygen molecule dissociates with a modest free-energy barrier even at room temperature, becoming the minimum (B) configuration. We have then found new reaction pathways in which the minimum (B) configurations are paired and the further backbond oxidation is facilitated. This finding is consistent with the layer-by-layer oxidation at the initial stage at room temperature observed by scanning reflection electron microscopy and Auger electron spectroscopy.[22]

IV. CONCLUSIONS

We have performed first-principles dynamical simulations for the first time that provide detailed atomistic reaction pathways and corresponding free-energy barriers in initial stages of Si oxidation. Our simulations clearly indicated the importance of the on-dimer structure. We also found that this structure is the trigger for sequential thermally activated dissociation of O_2 molecules. These reactions around on-dimer structures cause widespread backbond oxidation around the structure. We clarified the detailed mechanisms of this reaction from the electronic viewpoint. The obtained atomistic picture contributes to our understanding of oxidation processes in nature and also contributes to progress in atom-scale technology.

*koizumi@comas.t.u-tokyo.ac.jp

[1]S. Iwata and A. Ishizuka, J. Appl. Phys. **79**, 6653 (1996).

[2]S. K. Ghandhi, *VLSI Fabrication Principles, Silicon and Gallium Arsenide*, 2nd ed. (Wiley, Chichester, 1994).

[3]A. C. Richard Grayson *et al.*, Proc. IEEE **92**, 6 (2004).

[4]International Technology Roadmap for Semiconductors at [http://public.itrs.net].

[5]Clemens J. Först, Christopher R. Ashman, Karlheinz Schwarz, and Peter E. Blöchl, Nature (London) **427**, 53 (2004).

[6]H. Watanabe, M. Saitoh, N. Ikarashi, and T. Tatsumi, Appl. Phys. Lett. **85**, 449 (2004).

[7]A. Redondo, W. A. Goddard III, C. A. Swarts, and T. C. McGill, J. Vac. Sci. Technol. **19**, 498 (1981).

[8]I. P. Batra, P. S. Bagus, and K. Hermann, Phys. Rev. Lett. **52**, 384 (1984).

[9]Y. Miyamoto and A. Oshiyama, Phys. Rev. B **41**, 12680 (1990); **43**, 9287 (1991).

[10]K. Kato, T. Uda, and K. Terakura, Phys. Rev. Lett. **80**, 2000 (1998).

[11]K. Kato and T. Uda, Phys. Rev. B **62**, 15978 (2000).

[12]L. C. Ciacchi and M. C. Payne, Phys. Rev. Lett. **95**, 196101 (2005).

[13]R. Car and M. Parrinello, Phys. Rev. Lett. **55**, 2471 (1985).

[14]M. Sprik and G. Ciccotti, J. Chem. Phys. **109**, 7737 (1998).

[15]A. Laio and M. Parrinello, Proc. Natl. Acad. Sci. USA **99**, 12562 (2002).

[16]M. Iannuzzi, A. Laio, and M. Parrinello, Phys. Rev. Lett. **90**, 238302 (2003).

[17]M. Boero, A. Oshiyama, and P. L. Silvestrelli, Phys. Rev. Lett. **91**, 206401 (2003).

[18]K. Kamiya, M. Boero, M. Tateno, K. Shiraishi, and A. Oshiyama, J. Am. Chem. Soc. **129**, 9663 (2007).

[19]N. Troullier and J. L. Martins, Phys. Rev. B **43**, 1993 (1991).

[20]J. P. Perdew, K. Burke, and M. Ernzerhof, Phys. Rev. Lett. **77**, 3865 (1996).

[21]S. Nosé, Mol. Phys. **52**, 255 (1984); J. Chem. Phys. **81**, 511 (1984); W. G. Hoover, Phys. Rev. A **31**, 1695 (1985).

[22]H. Watanabe, K. Kato, T. Uda, K. Fujita, M. Ichikawa, T. Kawamura, and K. Terakura, Phys. Rev. Lett. **80**, 345 (1998).

[23]A. Laio and F. L. Gervasio, Rep. Prog. Phys. **71**, 126601 (2008).

[24]T. Uchiyama, T. Uda, and K. Terakura, Surf. Sci. **474**, 21 (2001).